LA-UR- 10-08305

Approved for public release; distribution is unlimited.

Title:	A PHOTOPHYSICAL STUDY OF TWO FLUOROGEN-ACTIVATING PROTEINS BOUND TO THEIR COGNATE FLUOROGENS
Author(s):	Tiziano Gaiotto, Hau B. Nguyen, Jaemyeong Jung, Andrew M. Bradbury, S. Gnanakaran, Jurgen G. Schmidt, Geoffrey S. Waldo, Peter M. Goodwin
Intended for:	Single Molecule Spectroscopy and Imaging IV (BiOS SPIE Photonics West) San Francisco, CA USA 1/22-27/2011

Form 836 (7/06)

A Photophysical Study of Two Fluorogen-Activating Proteins Bound to their Cognate Fluorogens

Tiziano Gaiotto, Hau B. Nguyen, Jaemyeong Jung, Andrew M. Bradbury, S. Gnanakaran, Jurgen G. Schmidt, Geoffrey S. Waldo, Peter M. Goodwin

ABSTRACT

We are exploring the feasibility of using recently developed fluorogen-activating proteins (FAPs) as reporters for single-molecule imaging. FAPs are single-chain antibodies choosen to specifically bind small chromophoric molecules termed fluorogens. Upon binding to its cognate FAP the fluorescence quantum yield of the fluorogen can increase substantially giving rise to a fluorescent complex. Based on the seminal work of Szent-Gyorgyi et al. (Nature Biotechnology, Volume 26, Number 2, pp 235-240, 2008) we have chosen to study two fluorogen-activating single-chain antibodies, HL1.0.1-TO1 and H6-MG bound to their cognate fluorogens, thiazole orange and malachite green derivatives, respectively. Here we use fluorescence correlation spectroscopy study the photophysics of these fluorescent complexes.

INTRODUCTION

Over the last 15 years, single-molecule imaging techniques has been broadly used to achieve important aims, providing molecular-level observation and insight of biological systems and biochemical reactions (Sako 2006), the study of single proteins or nucleic acids (Hegner 2002, Kaji 2007, Eydeler 2009), and the dynamics of both protein/DNA interactions and enzyme activity (Jahnz 2004, Yao 2006, Hilario 2010). With the purpose of depicting molecular states and dynamics, several different techniques have been applied, but optical methods are the most used for the high spatial and temporal resolution that can be achieved, including FRET (fluorescence resonance energy transfer), wide-field and confocal microscopy and FCS (fluorescence correlation spectroscopy) (Medina 2002, Haustein 2004, Rigler 2010).

When optical methods are performed, there are basically two aspects that must be evaluated for an accurate detection of a single-fluorescent molecule (in solution or within a living cell): 1) the selection of an appropriate fluorescent probe, and 2) the labeling system to use to link the probe to the molecule of interest. There is a wide range of different probes that can be used, and each one of them must be coupled to a carrier to allow the specific binding to the target molecule but it must not interfere with its activity features.

The labeling of monoclonal antibodies is a widespread method, where an antibody with a specific binding activity can be conjugated to a fluorescent reporter such as an organic fluorophore or a quantum dot for specific detection and imaging of the species of interest(Zhou 2006). It is also possible to express proteins or enzymes directly fused to the specific tags, as biotin (for fluorophores- or QD-conjugated streptavidin interactions), coiled-coil motifs or the recent Halotag (Promega). Another well-characterized approach is the ectopic expression of genetically fused fluorescent proteins, as green fluorescent protein (GFP) and its fragments (Cabantous 2005), to the protein of interest. In all these systems the activity of the fluorophore probes is usually not altered by the binding to target molecule ?NOT TRUE IN THE CASE OF SPLIT GFP?, and the probes are already fluorescent. In the Biarsenical system, non-fluorescent molecules (FIAsH and ReAsH) bind a small tetracysteine amino acid sequence (Adams 2002), generating a fluorescent-protein complex.

Szent-Gyorgyi and coworkers developed an alternative imaging system based on fluoromodules, a complex of fluorogenic dyes (fluorogens) and proteins or nucleic acids (Szent-Gyorgyi 2007): the fluorogen is only weakly fluorescent, but the interaction with a cognate protein (or FAP, fluorogen-activating protein) substantially enhances the fluorescence quantum yield of the fluorogen, and light emission is observed. In their work, the cognate protein is a single-chain antibody selected from a yeast-displayed human antibody library: they isolated single-chain fragments (~30 kDa) that recognize and bind with high affinity only the specific dye, used during selection steps. They performed the selection with two fluorogens, namely Thiazole Orange (TO) and Malachite Green (MG). After a further step of yeast affinity maturation to obtain improved binders, they isolated 3 single-chain antibodies against TO and 6 against MG. For the studies of this work, we chose the FAP with the highest fluorescence enhancement value for each fluorogen: HL1.0.1-TO1 and H6-MG.

The aim of this work is to evaluate these FAP/fluorogen complexes as fluorescent reporters for single molecule imaging. Here we use fluorescence correlation spectroscopy to measure characterize the HL1.0.1-TO/TO1-2p and

H6-MG/MG-2p complexes under excitation conditions similar to those required for single molecule spectroscopy and imaging.

MATERIALS AND METHODS

1. Construction of expressing vectors

The sequences of HL1.0.1-TO1 and H6-MG single-chain antibodies (from Sznet-Gyorgyi *et al.* paper [*Sznet-Gyorgyi et al.*]) were used for genes synthesis and *E.coli* codon optimization (GenScript USA Inc.). Both Sc-Fv cassettes were digested with BssHII-NheI restriction endonucleases from the pUC57 vector provided by GenScript, and subsequently subcloned into pEP-Ecoil vector [*Ayriss et al.*]. The final vectors, namely pEP-Ecoil HL1.0.1-TO1 and pEP-Ecoil H6-MG, were used to transform electrocompetent cells BL21: the colonies were sequenced and stocked at -80°C.

2. Expression and purification of soluble FAPs

BL21 single transformants were grown in 1 liter baffled-flasks with 100 ml of 2xYT media and 50 μg/ml Kanamicin at 37°C. At bacterial $O.D._{600}$ 0.5, the expression of the recombinant protein was induced with 0.2 mM IPTG for 16 h at 28°C. The periplasmic proteins were extracted following the protocol in Falco et al. [Falco et al.]. The single-chain antibodies were purified taking advantage of C-term His6-tag, by using Ni-NTA resin (Qiagen) and following the provided instructions. The proteins were subsequently eluted with 250 mM Imidazole buffer and dialyzed in phosphate buffer saline (PBS), overnight at 4°C. The concentration of each single-chain antibody was assessed with the Coomassie Plus Protein Assay (Thermo Scientific). The quality of purified proteins was verified running 500 ng of each samples in a SDS-PAGE electrophoresis gels: the proteins were transferred onto a nitrocellulose membrane (Whatman), and detected with 1 μg/ml mouse α-SV5 antibody and 1μg/ml goat α-mouse AP-conjugated antibody (SantaCruz).

3. FAPs-binding activity assay

500 ng of HL1.0.1-TO1 and H6-MG were mixed with 2 μM of thiazole orange-2p (TO1-2p) and malachite green-2p (MG-2p) respectively in 100 μl of wash buffer (0.2 mM EDTA, 0,1% Pluronic F-127 in 1x PBS). The diethylene glycol diamine dyes (TO1-2p, MG-2p) were kindly provided by Professor Alan Waggoner. The samples were assayed for fluorescence on a Tecan Infinite M200 reader: MG-2p was analyzed with 630nm excitation /685nm emission wavelength, TO-2p with 488nm excitation/535nm emission wavelength.

4. Fluorescence Correlation Spectroscopy

Fluorescence correlation spectroscopy was done using a modified inverted optical microscope (IX-71, Olympus-Japan). Continuous-wave laser excitation at either 488 nm (Sapphire 488HP, Coherent Inc.) or 633 nm (Melles Griot) was introduced through the arc-lamp port of the microscope. An excitation dichroic (XF2035, Omega Optical Inc. at 633 nm or 488DRLP-NIR, Chroma Technology Corp. at 488 nm) was used to reflect the excitation laser through the back aperture of a ×60, 1.2 NA water immersion objective (UPLSAPO 60XW, Olympus-Japan) and transmit the fluorescence emission collected by the same objective. A 50-μm diameter pinhole located in the image plane of the microscope camera port was used to spatially filter the collected emission. Under these conditions, the probed volume of solvent was ~1fL. An appropriate band pass filter (550/88 nm for HL1.0.1-TO/TO1-2p or 700/75 nm for H6/MG-2p) was used to spectrally filter the emission. The filtered emission was split with a 50%/50% beam splitter and imaged onto two single-photon counting avalanche photodiodes (APDs) (SPCM-AQRH, PerkinElmer). Short pass filters (Thorlabs) were placed in front of each APD to reject near-infrared APD-generated photoluminescence that would lead to spurious correlation artifacts at short lag times. The APD outputs were fed into a digital correlator (ALV GmbH, ALV 5000E/FAST) housed in a PC for the real-time calculation, display and storage of the intensity correlations. The intensity autocorrelation was obtained by cross-correlating the APD outputs to eliminate short lag-time artifacts due to APD detector dead time and after-pulsing. The dimensions of the 488-nm and 633-nm excited probe volumes were estimated from model fits of FCS curves recorded using calibration fluorophores (Rhodamine 110 (Rh110) at 488 nm and Cy5 at 633 nm) and estimates of the translational diffusion coefficients of these fluorophores in water (D_{Rh110} = 430 $\mu m^2/s$ (2), D_{Cy5} = 330 $\mu m^2/s$ (3)) at room temperature (20° C). Based on these calibration measurements, the lateral and axial dimensions of the 488 nm excited probe volume were: ω_1 = 0.28 μm and ω_2 = 1.5 μm, respectively; the dimensions of the 633 nm excited probe volume were: ω_1 = 0.32 μm, ω_2 = 2.1 μm. The aspect ratio of the probe volume (ω_2/ω_1), was 5.4 and 6.7 for the 488 nm and 633 nm excited probe volumes, respectively. Typically the FCS curves were collected in 5 runs of 120 seconds each. The FAP/fluorogen mixtures were made up in wash buffer (0.2 mM EDTA, 0,1% Pluronic F-127 in 1x PBS) adjusted to

pH 7 for the intensity dependence studies and 1X PBS with the pH adjusted over the range of 4 to 10 for the pH dependence study.

RESULTS

1. FAPs expression and dyes-binding activity assay

Two different fluorogen activating proteins were expressed and purified for the subsequent FCS analysis: the whole VH-VL single-chain HL1.0.1-TO1, which binds thiazole orange, and the single-VH domain H6-MG, which binds malachite green. The genes were synthesized and subcloned into a prokaryotic vector, pEP-Ecoil: the vector allows the expression of recombinant proteins coupled with the E coil domain, the SV5 tag and the Histidine tag (Figure 1).

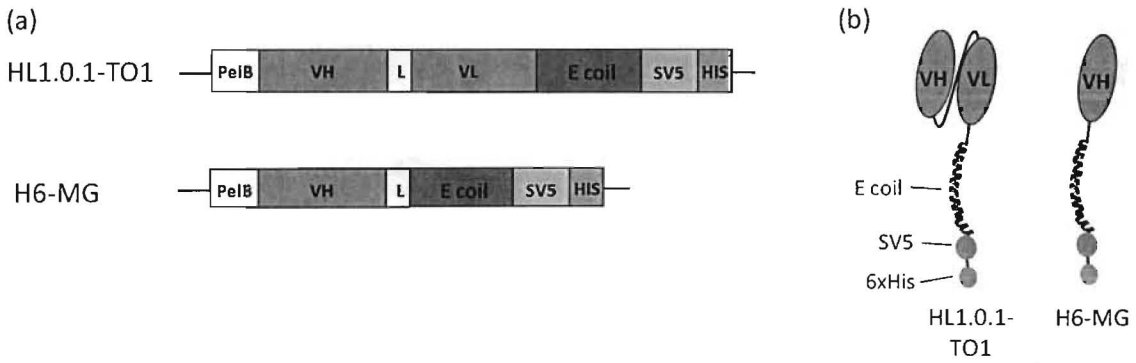

Figure 1. (a) Schematic representation of the expression cassettes of pEP-Ecoil vector for the expression of single-chain antibody fragments HL1.0.1-TO1 and H6-MG. The antibody fragments are cloned as N-terminal fusions with the E coil domain, the SV5 tag and the Histidine tag (6xHis). (b) Schematic representation of the recombinant antibody fragments illustrating the difference between the two antibody fragments. HL1.0.1-TO1 is a complete single chain, composed by a VH domain, a linker (L) and a VL domain. H6-MG is encoded by a single VH domain..

The protein expression is under the control of an IPTG-inducible promoter, and the PelB leader in the vector allows the protein translocation into the periplasmic space of bacteria. By using an osmotic shock extraction, it is possible to recover only the correctly folded single-chain antibodies from the periplasmic space, and to purify them using a Nickel resin that binds the His6-tag at the C-terminus. The results of the protein purification are reported in Figure 2a. The Immunoblot shows the size of recombinant HL1.0.1-TO1 and H6-MG, that agrees with their theoretical size, about 35 and 25 kDalton respectively.

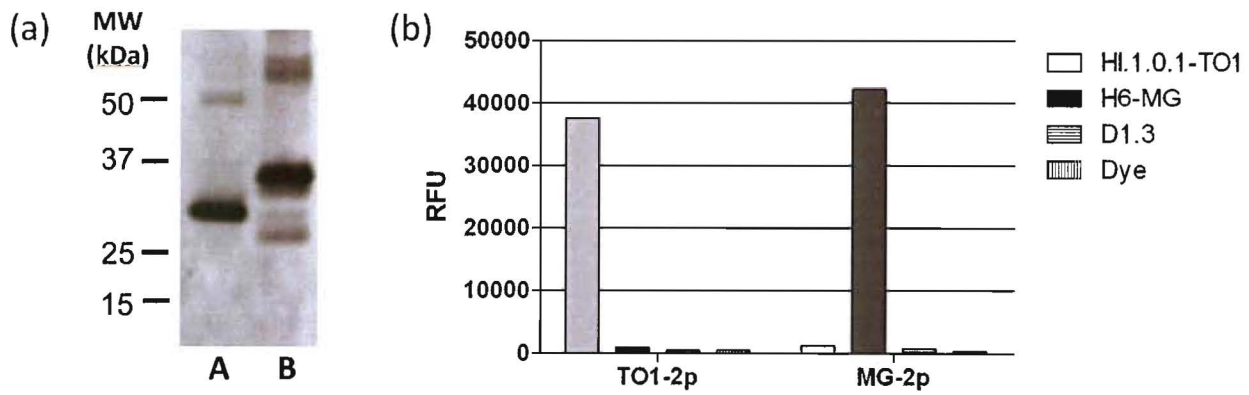

Figure 2. (a) TO FINISH

To verify the binding activity of the purified FAPs, we incubated them with the cognate dyes and after 1 hour we read the emission signal of each sample (Figure 2b). We performed the binding assay and the further studies with diethylene glycol diamine coupled fluorogens TO1-2p and MG-2p. The fluorescence signal of HL1.0.1-TO and H6-MG interactions agrees with the specificity of each FAP-dye pair: in fact the signal of the FAP interaction with the

non-cognate fluorogen is comparable with the negative controls we included in the assay (the fluorogen alone, and the interaction with the single-chain D1.3, an anti-lysozyme antibody).

2. Fluorescence Correlation Spectroscopy

FCS uses the normalized second order autocorrelation of the fluorescence intensity, $G(\tau) = 1+\langle\delta I(t+\tau)\delta I(t)\rangle/\langle I\rangle^2$, to probe temporal fluctuations in the fluorescence emission.(4) Here the angle brackets denote an average over time, t; $\delta I(t) = I(t)-\langle I\rangle$ and τ, the lag time. In principle, any molecular process that leads to a change in the fluorescence intensity can monitored by FCS over timescales ranging from nanoseconds to milliseconds. Such processes include translational and rotational diffusion, intersystem crossing between bright singlet and dark (e.g., triplet) states, and chemical reactions.

Our experimental results can be fitted using the following model(5):

$$G(\tau) = (1+\mathrm{R}e^{-\tau/\tau_R}) \times \prod_{i=0}^{i=1}\left[1+\frac{T_i}{1-T_i}e^{-\tau/\tau_i}\right] \times \frac{1}{N}(1+4D\tau/\omega_1^2)^{-1}(1+4D\tau/\omega_2^2)^{-1/2}+1 \qquad \text{Eq. (1)}$$

Here the first term of the product denoted with the pair of multiplication symbols (×) accounts for rotational diffusion of the excitation dipole moment of the fluorescent species. τ_R is the rotational correlation time and R is the amplitude of the rotational diffusion component. The second term is a product of two terms that account for transitions into and out of two non-fluorescent states with time constants τ_0 and τ_1 with associated mean fractions (T_0, T_1) of the fluorescent species within the probe volume in these states. The third term accounts for translational diffusion of the fluorescent species into and out of the probe volume. Here N is the average number of fluorescent molecules in the probe volume; ω_1 and ω_2 are the radial and axial dimensions of the probe volume, respectively; and D is the translational diffusion coefficient of the fluorescent species. The average time, τ_d, for the fluorescent species to diffuse across the radial dimension of the probe volume is $\omega_1^2/(4D)$.

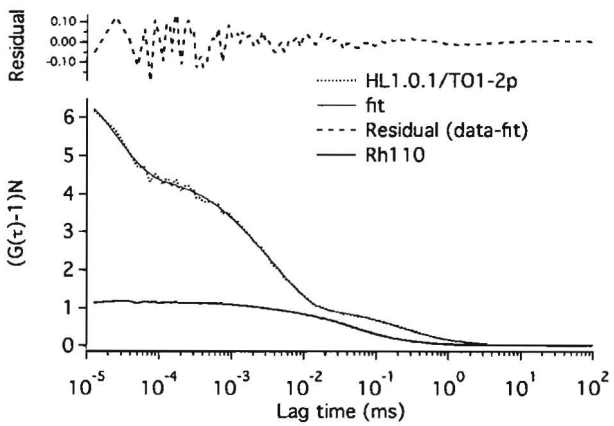

Figure 3. Intensity autocorrelations of the HL1.0.1-TO/TO1-2p complex (dotted curve) and Rhodamine 110 (Rh110) (solid curve) recorded using 50 μW of 488 nm excitation power (20 kW/cm^2). Autocorrelations are normalized to an average occupancy of one (N=1). The HL1.0.1-TO/TO1-2p FCS curve shows several decay processes: (i) a short-lived decay in the nanosecond range we attribute to rotational diffusion of the HL1.0.1-TO/TO1-2p complex; (ii) a two-component decay in the microsecond range reflecting fluorescence fluctuations from transitions into and out of dark states; and (iii) an overall decay (~200 μs) due to diffusion of the HL1.0.1-TO/TO1-2p complex across the probe volume. The Rh110 intensity autocorrelation shows a simpler form dominated by the diffusion of the Rh110 fluorophore across the probe volume (~50 μs). The faster (sub-nanosecond) rotational diffusion of the Rh110 fluorophore is not resolved in this experiment.

Figure 3 shows intensity autocorrelations recorded using 488 nm excitation from two samples containing ~100 nM HL1.0.1-TO FAP and 1 μM TO1-2p fluorogen (dotted curve), or ~10 nM Rh110 (heavy solid curve). Control experiments showed very low fluorescence from the HL1.0.1-TO FAP alone (5 kHz total count rate) and low fluorescence from the fluorogen alone (25 kHz total count rate). The mixture of the protein and fluorogen was substantially brighter giving a total count rate of 240 kHz. We therefore attribute the majority of the fluorescence from the mixture to a complex formed between the HL1.0.1-TO FAP and the fluorogen. The FCS curve for the HL1.0.1-TO/TO1-2p complex shows three readily discernable decay processes in the nanosecond to millisecond time range. The light solid curve overlaying the data is an un-weighted fit to the FCS data using Eq. 1 with the ratio of the axial and radial probe volume dimensions fixed at ω_2/ω_1 = 5.4. From the fit: τ_R = 26 ns; R = .65; τ_0 = 5.4 μs; T_0 = 0.71; τ_1 = 1.1 μs; T_1 = .23; and $\tau_d = \omega_1^2/(4D)$ = 200 μs. The measured rotational correlation time, 26 ns, is in the range expected for a protein the size of HL1.0.1-TO and indicates that, in the fluorescent complex, the fluorogen is tightly bound to the HL1.0.1-TO protein. The measured diffusion time, 200 μs, gives a diffusion coefficient of 100 μm^2/sec for the fluorescent complex. This is somewhat larger

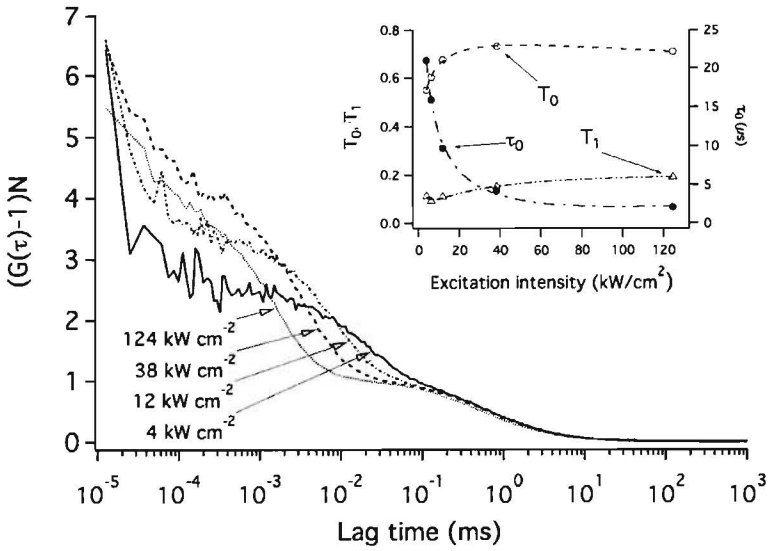

Figure 4. Intensity autocorrelations of the H6-MG/MG-2p complex recorded at four different 633 nm excitation intensities. The autocorrelations are normalized to an occupancy of one (N=1). The inset shows the excitation intensity dependence of the slow flicker time, τ_0, its fraction, T_0, and the fast flicker (τ_1 = 1.0 μs) fraction, T_1. Curves are drawn through the data points to guide the eye.

than that expected(6) for a 35 kDa protein, D = 75 μm^2/sec, that would give an average diffusion time of 260 μs in our setup. This discrepancy may be due to photobleaching of the fluorescent complexes as they diffuse across the probe volume resulting in a shortened apparent diffusion time.(7)

Figure 4 shows a set of intensity autocorrelations recorded from a sample containing ~1 μM H6-MG FAP and ~100 nM MG-2p fluorogen using a four 633 nm excitation intensities ranging from 4 to 124 kW/cm^2. The fluorescence intensity of either component alone was neglible compared to that of the mixture. We therefore attribute the fluorescence of the mixture to the H6-MG/MG-2p complex. For ease of comparison the FCS curves are normalized to an occupancy of one (N=1). As with HL1.0.1-TO/TO1-2p (see Figure 3), three decay processes are readily apparent in the FCS curve: a short-lived decay in the nanosecond range that we attribute to rotational diffusion of the H6-MG/MG-2p complex; a decay in the microsecond range due to transitions into and out of dark states; and an overall decay (~500 μs) due to diffusion of the H6-MG/MG-2p complex across the probe volume. The ~20 ns rotational correlation time indicates that the MG-2p fluorogen is tightly bound to the H6-MG FAP protein. As shown in the figure the FCS curves show an obvious dependence on the excitation intensity. The FCS curves were fit using Eq. 1. In these fits the aspect ratio of the probe volume, ω_2/ω_1, was fixed at 6.7. Two exponential 'flicker' processes in the microsecond time range were required to obtain good fits to the FCS curves. The time constant of the faster flicker component was constrained to τ_1 = 1.0 μs and its fraction, T_1, was allowed to vary. The slow flicker time, τ_o, and its fraction, T_1, were both allowed to vary. The rotational correlation time, τ_R, was constrained to 20 ns and its amplitude, R, was allowed to vary. The data were fit without weighting to facilitate the fitting of the short time range of the FCS curves. The inset in Figure 4 shows the excitation intensity dependence of the slow flicker time, τ_0, and the fast (T_1) and slow (T_0) flicker fractions. The diffusion times, τ_d, of the H6-MG/MG-2p complex obtained from the fits ranged from 440 μs to 550 μs. A reduction in the apparent diffusion time was observed with increasing excitation intensity and is likely due to photobleaching of the H6-MG/MG-2p complex. The diffusion time measured at low excitation intensity (550 μs) gives a diffusion coefficient of 47 μm^2/sec. Based on its molecular weight (25 kDa) one would estimate a diffusion coefficient of 84 μm^2/sec for the H6-MG/MG-2p complex. This is substantially larger than the measured value and leads us to conclude that the fluorescent complex is comprised of H6-MG/MG-2p multimers.

Figure 5 shows the pH-dependence of the H6-MG/MG-2p complex intensity autocorrelations. The FCS curves were fit to Eq. 1 using the procedure outlined for the excitation intensity dependence study shown in Figure 4. As shown in the inset of Figure 5, the slow flicker fraction, T_0, shows a clear pH-dependence, decreasing from ~0.8 to ~0.5 as the pH is increased from 4 to 10. The slow flicker time, τ_0, does not show a significant pH dependence. The fast flicker fraction, T_1, shows a gradual increase as the pH is increased from 4 to 10.

Figure 6 shows the molecular brightness of the HL1.0.1-TO/TO1-2p and H6-MG/MG-2p complexes as a function of excitation intensity. The molecular brightness of the FAP/fluorogen complex is obtained by dividing the fluorescence intensity (total count rate) by the average occupancy (N) obtained from the FCS curve. For HL1.0.1-

TO/TO1-2p a peak molecular brightness of ~2 kHz per complex was obtained at a 488 nm excitation intensity of 10 kW/cm^2. The HL1.0.1-TO/TO1-2p emission is completely saturated at excitation intensities above ~10 kW/cm^2. As a comparison, the calibration fluorophore, Rh110, has a molecular brightness of ~50 kHz per fluorophore when excited at 10 kW/cm^2. The H6-MG/MG-2p complex is substantially brighter than HL1.0.1-TO/TO1-2p, attaining a molecular brightness of ~20 kHz per complex at a 633 nm excitation intensity of ~120 kW/cm^2. This is still substantially less than Cy5, which has a molecular brightness of ~170 kHz per fluorophore when excited at ~120 kW/cm^2.

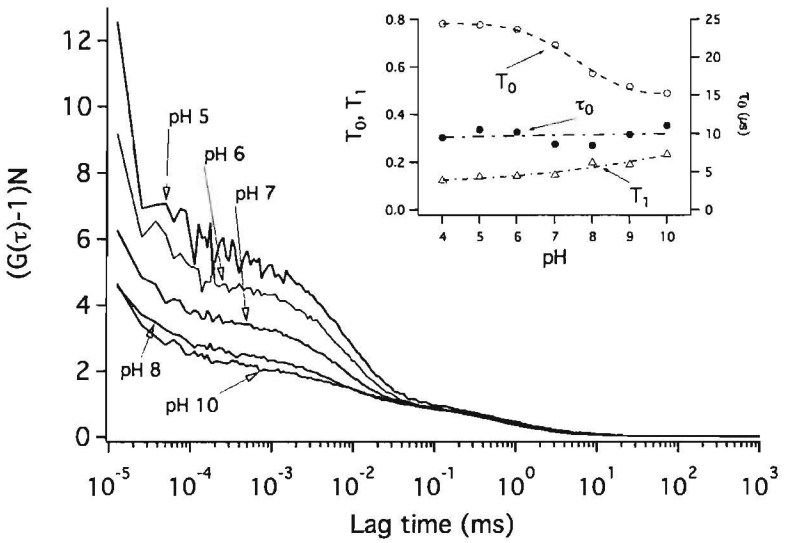

Figure 5. pH dependence of the H6-MG/MG-2p complex intensity autocorrelation. Fluorescence was excited at 633 nm (12 kW/cm^2). The autocorrelations are normalized to an occupancy of one (N=1). The inset shows the pH-dependence of the slow flicker time, τ_0, its fraction, T_0, and the fast flicker (τ_1 = 1.0 μs) fraction, T_1. Curves are drawn through the data points to guide the eye.

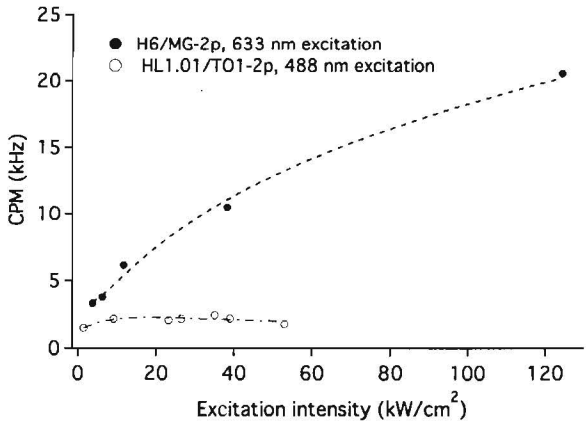

Figure 6. HL1.0.1/TO1-2p (open circles) and H6/MG-2p (solid circles) complex brightness as a function of excitation intensity. These values were obtained by dividing the total fluorescence count rate by the average occupancy (N) in the probe volume obtained from a fit to the intensity autocorrelation function. Curves are drawn through the data points to guide the eye.

DISCUSSION

The FCS curves from both FAP/fluorogen complexes show three readily apparent decay processes in the nanosecond to millisecond range. We attribute the shortest, ~20 ns, decay time to fluorescence fluctuations due to rotational diffusion of the fluorogen dipole moment. This long rotational correlation time is in the range expected for the FAP proteins and indicates that, in the fluorescent complex, the fluorogens are tightly bound to the body of the FAP protein. Both the HL1.0.1-TO/TO1-2p and H6-MG/MG-2p complexes exhibit two discernable 'flicker' processes in the microsecond time-range that we attribute to transitions into and out of non-fluorescent states. We carried out FCS measurements of the H6-MG/MG-2p complex as a function of excitation intensity and pH to explore the dependence of the microsecond flicker processes on these parameters. The most prominent of these flicker processes has a time-constant, τ_0 that decreases from ~20 to ~2 microseconds and a dark fraction, T_0, that increases from ~0.5 to ~0.7 as the excitation intensity is increased from ~4 to ~120 kW/cm^2. A second flicker component with a time constant τ_1 ~ 1 μs and a smaller dark fraction, T_1, that increases with excitation intensity from ~0.1 to ~0.2 was also detected.

The pH-dependence of the H6-MG/MG-2p fluorescence correlation spectra is manifested primarily as a decrease in the slow flicker dark fraction, T_0, from ~0.8 to ~0.5 as the pH is increased from 4 to 10. The slow flicker time (τ_0 ~ 10μs) does not vary significantly with pH. The fast flicker fraction, T_1, increases

from ~0.1 to ~0.2 as the pH is increased from 4 to 10.

The low saturation intensities exhibited by both of the FAP/fluorogen complexes (Figure 6) are consistent with the large dark fractions seen in their fluorescence correlation spectra and the intensity dependence of the H6-MG/MG-2p slow flicker dark fraction, T_0. The pH dependence of the H6-MG/MG-2p slow flicker fraction indicates that the

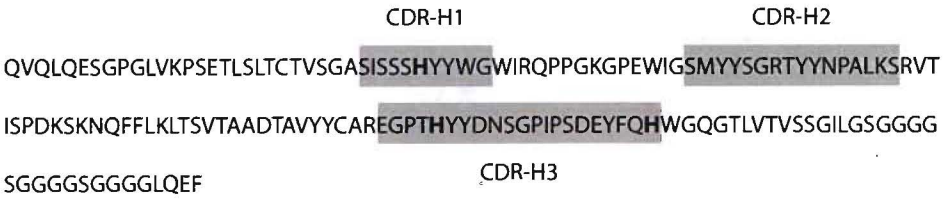

Figure 6. H6-MG peptide sequence(1) with the three putative complementary determining regions (CDR-H1, CDR-H2, CDR-H3) highlighted in grey. Histidine residues located in the CDRs are in boldface type.

local environment of the FAP-bound fluorogen changes near pH7. A Kabat analysis(8) of the H6-MG peptide sequence (Figure 6) shows that three histidine residues are located in the complementary determining regions (CDR) that presumably form the fluorogen binding pocket. Ionization of one or more of these histidine residues (pKa ~ 6) with increasing pH may alter the local environment of the bound fluorogen leading to changes in the photophysics of the MG-MG/MG-2p complex.

SUMMARY

We have performed FCS measurements on two FAP/fluorogen complexes, HL1.0.01-TO/TO-2p and H6-MG/MG-2p. Fluorescence intensity autocorrelations from both of these fluorescent complexes show photodynamic 'flicker' processes in the microsecond range with substantial dark fractions. These flicker processes cause the fluorescence emission from these complexes to saturate at relatively low excitation intensities. The H6-MG/MG-2p dark fraction decreases as the pH is increased from 4 to 10. This may be due to the ionization of one or more histidine residues present in the putative fluorogen binding pocket of H6-MG. The longer than expected crossing time of the H6-MG/MG-2p complex leads us to believe that it is multimeric.

(1) C Szent-Gyorgyi, BA Schmidt, Y Creeger, GW Fisher, KL Zakel, S Adler, JAJ Fitzpatrick, CA Woolford, Q Yan, KV Vasilev, PB Berget, MP Bruchez, JW Jarvik, A Waggoner: Fluorogen-activating single-chain antibodies for imaging cell surface proteins. Nature Biotechnology 26 (2008) 235-40.

(2) PO Gendron, F Avaltroni, KJ Wilkinson: Diffusion Coefficients of Several Rhodamine Derivatives as Determined by Pulsed Field Gradient-Nuclear Magnetic Resonance and Fluorescence Correlation Spectroscopy. Journal of Fluorescence 18 (2008) 1093-101.

(3) A Loman, T Dertinger, F Koberling, J Enderlein: Comparison of optical saturation effects in conventional and dual-focus fluorescence correlation spectroscopy. Chemical Physics Letters 459 (2008) 18-21.

(4) A Van Orden, K Fogarty, J Jung: Fluorescence fluctuation spectroscopy: A coming of age story. Applied Spectroscopy 58 (2004) 122A-37A.

(5) J Widengren, B Terry, R Rigler: Protonation kinetics of GFP and FITC investigated by FCS - aspects of the use of fluorescent indicators for measuring pH. Chemical Physics 249 (1999) 259-71.

(6) ME Young, PA Carroad, RL Bell: Estimation of diffusion coefficients of proteins. Biotechnology and Bioengineering 22 (1980) 947-55.

(7) ST Hess, SH Huang, AA Heikal, WW Webb: Biological and chemical applications of fluorescence correlation spectroscopy: A review. Biochemistry 41 (2002) 697-705.

(8) EA Kabat, TT Wu, M Reid-Miller, H Perry, K Gottesman, Sequences of proteins of immunological interest, Report # 165-492. U.S. Government Printing Office, Bethesda, MD, 1983.